Available online at www.sciencedirect.com
ScienceDirect
Journal of Molecular Spectroscopy 245 (2007) 89–99
Journal of MOLECULAR SPECTROSCOPY
www.elsevier.com/locate/jms

High sensitivity ICLAS of D_2O between 12450 and 12850 cm^{-1}

A. Campargue [a,*], F. Mazzotti [a], S. Béguier [a], O.L. Polyansky [b,d], I.A. Vasilenko [c], O.V. Naumenko [c]

[a] *Laboratoire de Spectrométrie Physique (associated with CNRS, UMR 5588), Université Joseph Fourier de Grenoble, B.P. 87, 38402 Saint-Martin-d'Hères, Cedex, France*
[b] *Institute of Applied Physics of Russian Academy of Sciences, 46, Uljanova Street, Nizhniy Novgorod 603950, Russia*
[c] *Institute of Atmospheric Optics, Russian Academy of Sciences, Tomsk 634055, Russia*
[d] *Department of Physics and Astronomy, University College London, London WC1E 6BT, UK*

Received 4 June 2007; in revised form 28 June 2007
Available online 26 July 2007

Abstract

The weak absorption spectrum of dideuterated water, D_2O, has been recorded between 12450 and 12850 cm^{-1} by high sensitivity Intracavity Laser Absorption Spectroscopy (ICLAS). This spectral region corresponds to the $(v_1 + v_2/2 + v_3) = 5$ polyad, dominated by the $4v_1 + v_3$ band centered at 12743.035 cm^{-1}. The achieved sensitivity has allowed for the detection of lines with a minimum intensity of 2×10^{-28} cm/molecule i.e. typically two orders of magnitude lower than previous observations in the region considered. A total of 586 energy levels belonging to 11 vibrational states were determined. The rovibrational assignment process of 1025 lines ascribed to D_2O was based on new results of variational calculations by Shirin et al. [S.V. Shirin, N.F. Zobov, O.L. Polyansky, J. Quant. Spectrosc. Radiat. Transfer, in press, doi:10.1016/j.jqsrt.2007.07.010]. The overall agreement between these calculations and the observed spectrum is good both for the line positions and line intensities. The difficulties encountered while performing the rovibrational labeling and the assignment of the weakest transitions not included in Combination Differences relations, are discussed.

Keywords: Deuterated water (D_2O); Intracavity Laser Absorption Spectroscopy (ICLAS); Rovibrational assignment

1. Introduction

In our preceding contribution [1], the weak absorption spectrum of dideuterated water, D_2O, was investigated by Intracavity Laser Absorption Spectroscopy (ICLAS) between 11400 and 11900 cm^{-1}. This spectral region corresponds to the $(v_1 + v_2/2 + v_3) = 4.5$ polyad dominated by the $3v_1 + v_2 + v_3$ and $v_1 + v_2 + 3v_3$ bands centered at 11500.25 and 11816.64 cm^{-1}, respectively. The present analysis is devoted to the $(v_1 + v_2/2 + v_3) = 5$ polyad lying in the 12450–12850 cm^{-1} region which is the highest energy polyad reported so far for D_2O. The $4v_1 + v_3$ band which corresponds roughly to the $\Delta v_{OD} = 5$ stretching overtone is centered at 12743.035 cm^{-1} and dominates the spectrum. One hundred and ninety-six lines in the central part of the investigated region (12553–12812 cm^{-1}) were previously recorded by ICLAS associated with a FTS detection scheme [2]. We are also aware that the absorption spectrum of D_2O in a wider region has been recently recorded by Fourier Transform Spectroscopy (FTS) with a 600 m path length in a Reims–Brussels collaboration [3]. One hundred and forty-two D_2O lines were detected by FTS in our region of interest (all lying between 12577 and 12815 cm^{-1}) while we could observe more than 1025 D_2O lines with our ICLAS spectrometer. The FTS line positions of Ref. [3] were used for wavenumber calibration of our ICLAS spectra (see below).

The $\Delta v_{OD} = 5$ stretching overtone of D_2O coincides approximately with that of HDO and has a band intensity about twice as large (for the pure species). The overview of the D_2O, HDO, and H_2O spectra in the region of interest

* Corresponding author. Fax: +33 4 76 63 54 95.
E-mail address: Alain.Campargue@ujf-grenoble.fr (A. Campargue).

0022-2852/$ - see front matter © 2007 Elsevier Inc. All rights reserved.
doi:10.1016/j.jms.2007.07.003

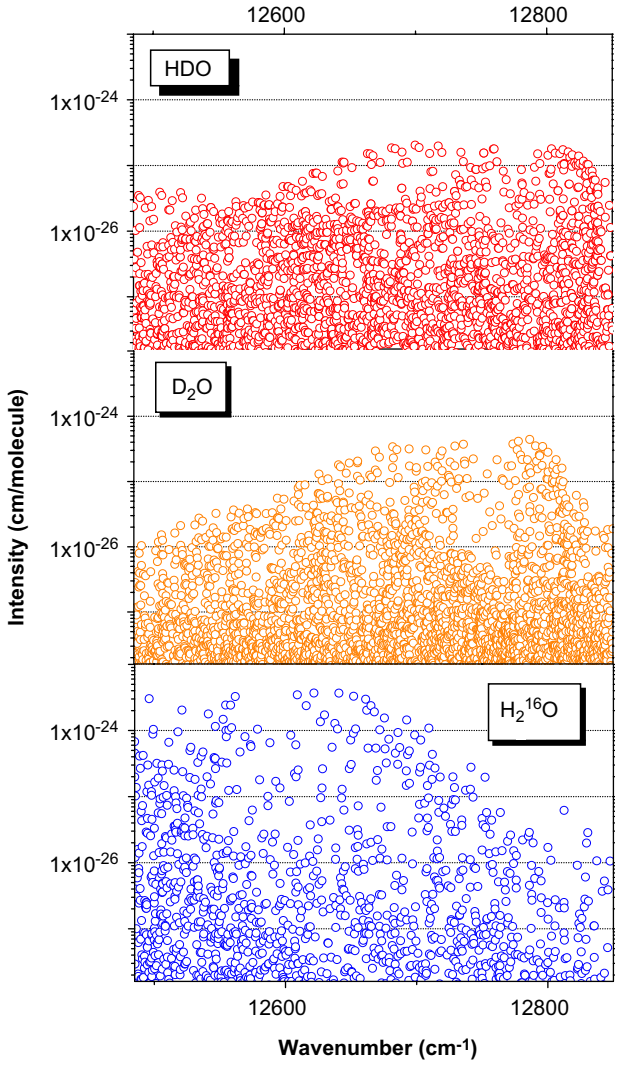

Fig. 1. Overview of the D_2O spectrum between 12450 and 12850 cm^{-1} as calculated by Shirin et al. [12] compared to the HDO and H_2O spectra calculated by Schwenke and Partridge [10,11]. Note the logarithmic scale adopted for the line intensity values. The line intensities correspond to the pure species.

(Fig. 1) shows that, below 12700 cm^{-1}, the $H_2{}^{16}O$ lines are stronger by up to two orders of magnitude compared to D_2O or HDO transitions. However no $H_2{}^{16}O$ lines were identified in our ICLAS spectra indicating that the deuterium enrichment of our gas sample was close to 100%, which constitutes an important advantage for the spectral analysis.

2. Experimental details

Our ICLAS experimental apparatus, based on a multimode Ti/Sapphire laser, has been previously described [4,5] and the experimental procedure adopted for the spectra recordings can be found in Ref. [1]. The intracavity sample cell was filled with D_2O (Aldrich, 99.96% D) at pressures up to 20 hPa. The spectra were recorded with a generation time of 150 μs corresponding to an equivalent absorption path length of 14.4 km. The experimental procedure consisted in successively filling the cell with water, recording the spectrum, evacuating the cell and recording the background spectrum. This procedure increases the signal to noise ratio (see Ref. [6]) and washes out natural water from the cell, leading to very high deuterium enrichment. From the absorbance of HDO transitions detected near 12800 cm^{-1}, we estimated the relative concentration of HDO and D_2O to be 2 and 98%, respectively, $H_2{}^{16}O$ concentration being negligible. An example of spectrum is displayed in Fig. 2.

The wavenumber calibration of each 12 cm^{-1} wide spectrum required the use of reference lines. In the 12610–12830 cm^{-1} region, FTS line positions as obtained from Ref. [3] were adopted. In the 12485–12610 and 12830–12850 cm^{-1} regions, we used D_2O lines identified in a ICLAS spectrum of a $D_2O/HDO/H_2O$ mixture recorded separately and calibrated against H_2O line positions from Ref. [7]. We found that the adopted indirect calibration procedure together with the uncertainty on the FTS wavenumber values of Ref. [3] limited the accuracy of our wavenumber values to about 5×10^{-3} cm^{-1} on average and in a few particular spectral sections, we could not rule out uncertainties as large as 8×10^{-3} cm^{-1}.

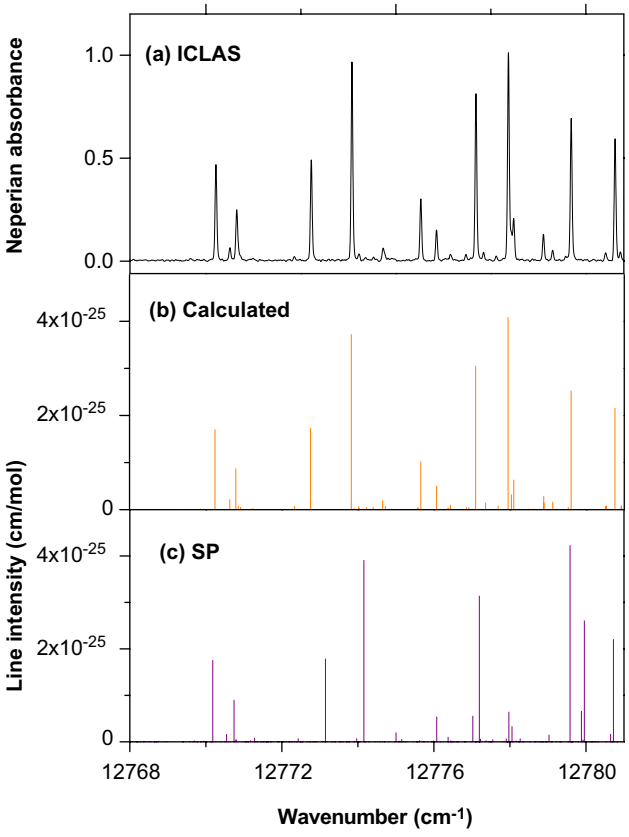

Fig. 2. Comparison of the D_2O spectrum around 12773 cm^{-1}: (a) ICLAS spectrum ($P \approx 20$ hPa, $l_{eq} \approx 14.4$ km), (b) results of the new variational calculations of Ref. [12], (c) results of the calculations of Schwenke and Partridge [10,11].

For each individual spectrum, a line list was created containing the line centers and the corresponding relative intensities obtained by fitting the line contour as a single Gaussian profile. We then applied a multi-Gaussian fit procedure in specific spectral sections which showed blended lines in order to retrieve more accurate relative line intensities. The retrieved values were then scaled against the values predicted by the new variational calculations presented below. The global line list was obtained after averaging the lines appearing in various recordings of the same spectral window, and in overlapping regions. We decided to consider two lines as identical when both their wavenumber difference was less than 0.008 cm^{-1}, and their intensity differed by at most a factor of 2. This global line list was then cleaned of spurious lines, or irreproducible spectral features close to the noise level. HDO lines were identified and removed by comparison with the line list attached to Ref. [8]. It leads to a list of 1045 transitions, which is the one considered in the following rovibrational analysis. The comparison of our line list with the FTS results of Ref. [3] is illustrated in Figs 3–5 for the whole investigated region and two specific spectral regions. The achieved sensitivity has allowed for the detection of lines with a minimum intensity of 2×10^{-28} cm/molecule i.e. typically two orders of magnitude lower than previous observations in the considered region [2,3].

A final comment concerns our experimental intensity values. The indirect procedure described above may lead to inaccurate values in particular for the weakest or blended lines. However, these values proved to be highly valuable for the rovibrational assignment, and they are given as estimated values in the line list attached as Supplementary Material.

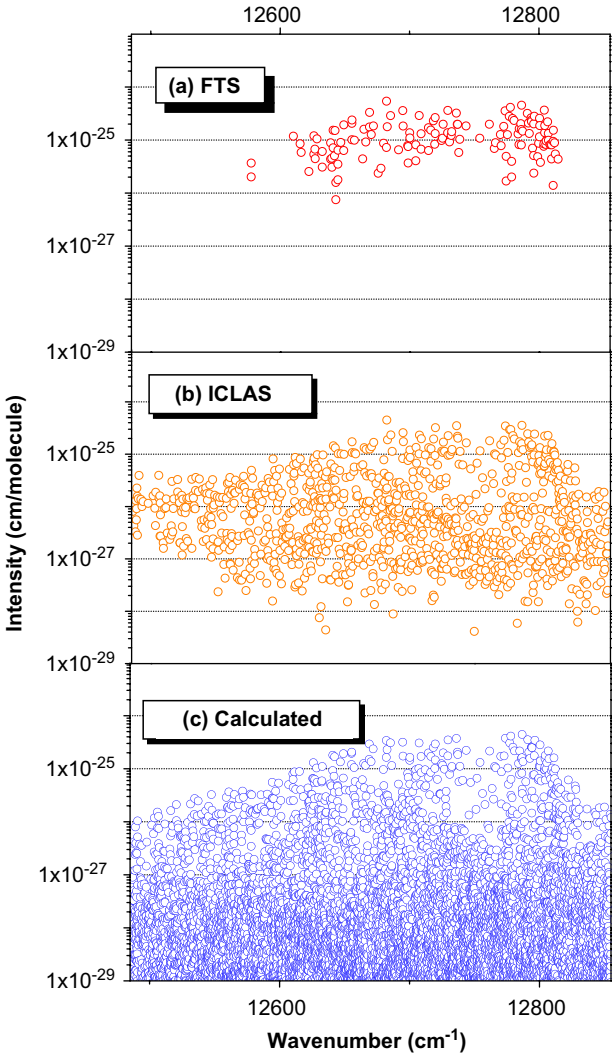

Fig. 3. Overview of the D_2O spectrum between 12450 and 12850 cm^{-1} (a) FTS [3], (b) ICLAS, (c) results of the new variational calculations of Ref. [12]. Note the logarithmic scale adopted for the line intensity values. The line intensities correspond to the pure species.

3. Rovibrational analysis

3.1. General procedure

The D_2O spectrum consisted of 1045 spectral lines including very weak absorption features. At the first stage of the analysis, the identification process was based on the results of the D_2O variational calculations of Ref. [9]. These calculations were performed by using the Potential Energy Surface (PES) optimized through the fitting to the experimental energy levels available at that time and on the Dipole Moment Surface (DMS) of Ref. [10]. They were found to improve significantly the well known predictions of Schwenke and Partridge (SP) [10,11]. However, as in our previous study [1], we evidenced large deviations (up to 1.3 cm^{-1}), for the energy levels of some vibrational states such as the (222) state. Such large differences prevented for the assignment of weak lines which are not involved in Ground State Combination Difference (GSCD) relations. For this reason, a new optimization of the D_2O PES was undertaken very recently [12] by enlarging the set of experimental energy levels of the D_2O molecule, with the results of the present study together with other recent studies (see Ref. [12] for details). The new D_2O PES has been derived using the *ab initio* surface, based on the calculations given in the archive attached to Ref. [13], as a starting point. The 27 morphing constants have been fitted to 1140 experimental energy levels with $J = 0$, 2, and 5 to minimize the standard deviation between the observed and the calculated energy levels. As a result, an rms value (0.023 cm^{-1}) close to the experimental accuracy was achieved for the residuals of the considered energy levels. As showed below and in Ref. [1], the quality of this new D_2O PES was found to be very good in the spectral region under study, with average and maximum (obs. − calc.) values of 0.06 and 0.27 cm^{-1}, respectively. This allowed us to identify 1025 (98%) of the experimental lines leaving 20 lines unassigned. The comparisons included in Figs 2–5 show the improved agreement with the experimental spectrum achieved by these new calculations compared to SP predictions.

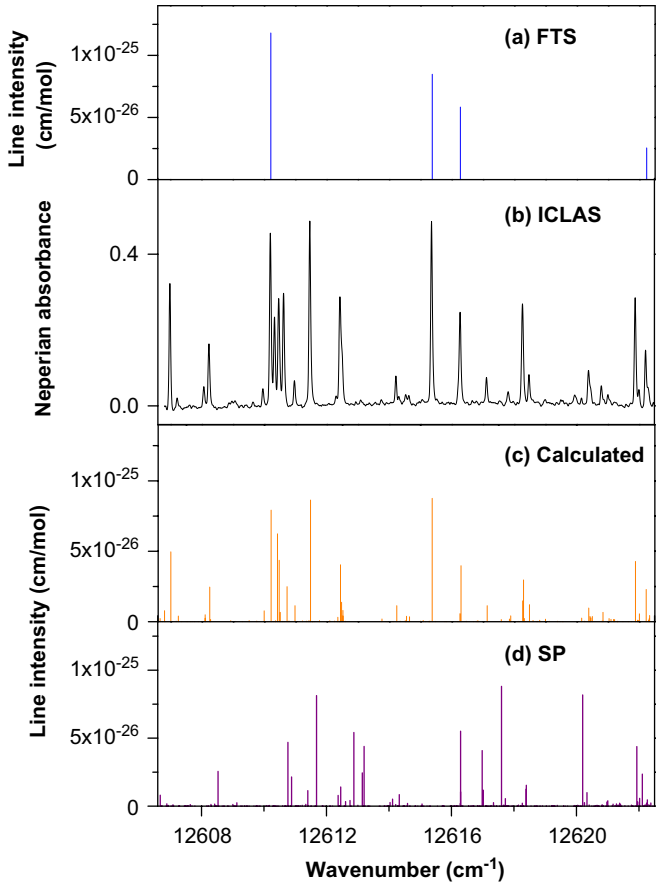

Fig. 4. Comparison of the D_2O spectrum around 12615 cm^{-1}: (a) FTS stick spectrum [3], (b) ICLAS spectrum ($P \approx 20$ hPa, $l_{eq} \approx 14.4$ km), (c) results of the new variational calculations of Ref. [12], (d) results of the calculations of Schwenke and Partridge [10,11].

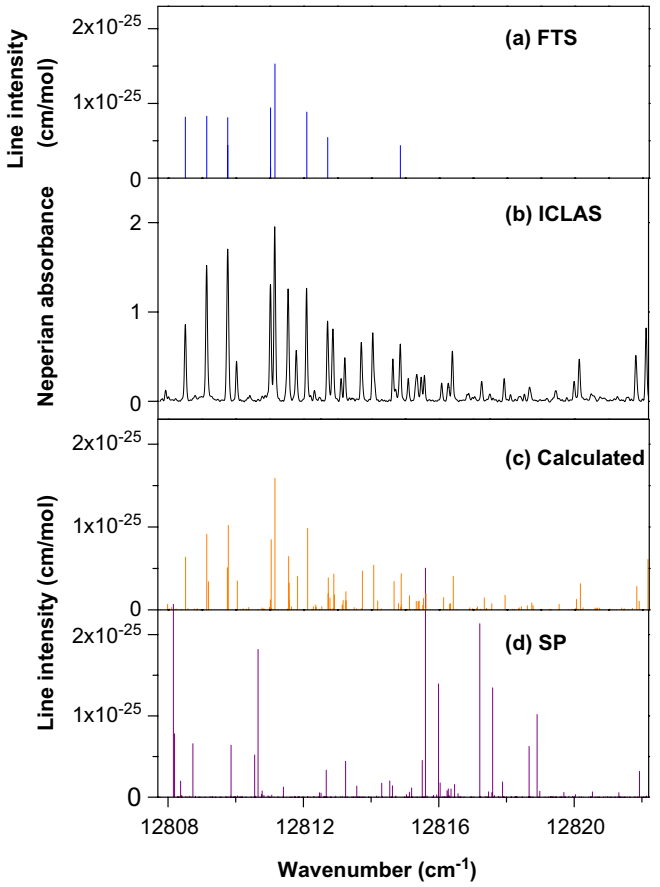

Fig. 5. Comparison of the D_2O spectrum in the region of the band head of the $4\nu_1 + \nu_3$ band around 12815 cm^{-1}: (a) FTS stick spectrum [3], (b) ICLAS spectrum ($P \approx 20$ hPa, $l_{eq} \approx 14.4$ km), (c) results of the variational calculations of Ref. [12], (d) results of the calculations of Schwenke and Partridge [10,11].

The summary of the retrieved experimental information is presented in Table 1 along with previous results [2,3]. The total number of energy levels (586) exceeds greatly those of Ref. [2] and Ref. [3] (66 and 85 levels, respectively). The retrieved experimental energy levels belong to a total of 11 vibrational states and are presented in Table 2 for the (401), (321), and (500) states, and in Table 3 for the (420), (222), (123), (043), (142), (302), (411) and (241) states. The deviations of the observed energy levels from the predicted values [12] are included in these Tables and plotted in Fig. 6. Energy levels, derived from blended lines, and, consequently, with lesser accuracy are marked by "B" in Tables 2 and 3.

Table 1
Summary of the spectroscopic information obtained by ICLAS for D_2O in the 12485–12853 cm^{-1} region

$\nu_1\nu_2\nu_3$	Band origin (cm^{-1})		Number of levels		
	Calc. [12]	Obs.	This work	Ref. [2]	Ref. [3]
241	12378.45		9		
142	12530.77		22		
420	12603.55		33		
321	12618.92	12618.912	163	1	8
043	12698.51		24		
500	12737.42	12737.397	97	5	3
401	12743.03	12743.035	162	60	74
222	12799.14	12799.25[a]	29		
123	12934.10	12934.22[a]	22		
302	12988.32	12988.42[a]	18		
411	13876.05		7		

[a] Value extrapolated from the [J0J] energy levels.

3.2. Rovibrational labeling

The rovibrational labeling of the observed energy levels assigned on the basis of variational calculations is often a laborious task. This was particularly the case in the present analysis as the variational calculations of Ref. [12] did not provide consistent rovibrational assignments for all of the energy levels involved. In Ref. [12], the quantum numbers were ascribed by an automatic procedure which is based on the smooth dependence of the rotational energies on the rotational quantum numbers [14]. Thus, the resulting labeling relies greatly on the assignment of the known experimental energy levels (which are believed to be correct). Consequently, as a result of a lack of experimental

Table 2
$D_2{}^{16}O$ rovibrational energy levels of the (401), (321), and (500) vibrational states derived from the ICLAS spectrum recorded between 12450 and 12850 cm^{-1}

J	K_a	K_c	(401)				(321)				(500)			
			E_{obs}	σ	N	Δ	E_{obs}	σ	N	Δ	E_{obs}	σ	N	Δ
0	0	0	12743.0350		1	14	12618.9120		1	−8	12737.3976		1	−16
1	0	1	12754.2638	1.7	2	11	12630.6555	0.5	2	−10	12748.8568		1	−8
1	1	1	12761.5176	0.2	2	15	12639.8043	4.0	2	−8	12756.1718	4.7	2	−8
1	1	0	12763.9136	0.5	2	14	12642.4733	0.1	2	−8	12758.3100		1	−13
2	0	2	12775.7040	0.9	2	−1	12653.5194	2.1	2	−13	12771.2596	3.5	2	−5
2	1	2	12781.9348	1.4	3	15	12660.3124	1.6	3	−8	12777.6237	2.3	3	8
2	1	1	12789.0847	1.6	4	14	12668.2220	1.3	2	−12	12783.5533	2.7	2	−3
2	2	1	12810.2854	0.8	3	11	12696.0241	0.9	2	3	12804.9408		1	−7
2	2	0	12810.8021	1.1	2	8	12696.5214	1.1	2	2	12805.4036		1	−5
3	0	3	12809.7130	0.9	3	8	12686.5734	3.0	3	−17				
3	1	3	12812.3211	1.3	3	8	12690.8690	0.8	3	−10	12806.4984	2.8	2	−7
3	1	2	12826.4351	1.6	3	8	12706.3795	1.5	2	−20	12821.0380		1	−9
3	2	2	12844.4756	3.8	3	7	12730.7408	0.7	2	2	12839.4028	3.1	2	−10
3	2	1	12846.9030	1.1	3	9	12733.1039	1.4	3	−3	12841.5984		1	−7
3	3	1	12886.1341	2.3	2	1	12783.3756	2.6	2	14				
3	3	0	12886.2036	3.3	2	2	12783.4426	1.1	2	22	12880.9005		1	−4
4	0	4	12851.2083	0.2	2	7	12728.9268	0.2	2	−17	12845.4142	1.6	2	−5
4	1	4	12852.4625	1.8	4	10	12731.2471	3.2	2	−16	12846.7970	0.8	3	−13
4	1	3	12875.3804	2.5	4	5	12756.1763	1.4	2	−29	12870.2697	0.6	2	−19
4	2	3	12889.6387	0.5	3	6	12776.6385	1.3	3	−7	12884.9785	0.2	2	−11
4	2	2	12896.1543	1.3	3	7	12783.1122		1	−11	12890.7971	1.3	2	−14
4	3	2	12932.2508	1.7	4	−2	12830.5128	0.8	3	17	12927.5826[B]	7.8	2	1
4	3	1	12932.7230	1.9	3	−3	12830.9154	1.9	2	13	12927.9677	2.5	3	−9
4	4	1	12989.1872	9.5	2	1	12901.9065		1	47	12984.3249		1	−16
4	4	0	12989.1910[B]		1	−3	12901.9008[B]		1	31	12984.3475		1	5
5	0	5	12901.6039	2.7	3	2	12780.1090	2.8	3	−22	12895.9081	7.4	2	−13
5	1	5	12902.1145	2.2	3	9	12781.1818	0.1	2	−21	12896.5013	0.2	3	−14
5	1	4	12934.9640	1.8	4	1	12822.6911	2.0	3	−43	12930.4275		1	−4
5	2	4	12945.4670	1.0	4	2	12833.3552	0.9	2	−26	12941.4536	1.5	3	−6
5	2	3	12958.4280	1.3	4	−1	12846.6159	1.2	3	−29	12953.4814	1.3	3	5
5	3	3	12990.4689	1.3	3	1	12889.3903	2.4	2	7	12985.9873	0.6	2	−18
5	3	2	12992.2637	2.6	4	−3	12890.9041	0.8	2	−8	12987.5311	2.9	2	−20
5	4	2	13047.4065	0.3	2	−3	12960.8986	3.9	2	31	13042.8316	3.1	2	−15
5	4	1	13047.4748	1.6	3	−1	12960.9466	1.5	4	40	13042.8928	1.4	2	−15
5	5	1	13120.4578		1	−1	13050.5406		1	62	13115.7453	1.9	2	−10
5	5	0	13120.4567	0.6	2	1	13050.5401		1	63	13115.7415		1	−14
6	0	6	12960.8874	0.7	2	5	12839.9262		1	−28	12955.2215		1	−15
6	1	6	12961.2754	1.5	3	5	12840.4270	0.2	2	−25	12955.4785		1	−20
6	1	5	13003.9492	0.1	2	−10	12893.3071	2.1	2	−41	13000.5091	1.7	3	−17
6	2	5	13011.6396	3.0	4	6	12900.7759	0.6	2	−26	13008.6896	1.2	3	−3
6	2	4	13033.8708	0.6	4	7	12923.0679	1.5	2	−47	13028.5893	2.5	2	−20
6	3	4	13060.0903	1.3	3	−5	12959.6643	0.3	3	−15	13055.9756	1.6	2	−14
6	3	3	13064.9069	0.4	2	−4	12963.6941[B]	2.2	2	−27	13060.1724	0.8	3	−21
6	4	3	13117.4911	0.3	2	−9	13031.8941	1.5	4	20	13113.2116	2.7	2	−20
6	4	2	13117.8196	1.5	3	1	13031.7499	2.5	4	7	13113.5057	0.1	2	−16
6	5	2	13190.4183[B]	1.9	2	−2	13121.3242	0.8	2	56	13186.0897		1	−16
6	5	1	13190.4157[B]	1.1	2	−12	13121.3216	2.2	2	58	13186.0813		1	−27
6	6	1	13281.3580	1.7	2	−7	13227.0727		1	82				
6	6	0	13281.3582	1.9	2	−7	13227.0731		1	82				
7	0	7	13028.9486	1.1	3	−4	12908.5883	0.2	3	−34	13023.4246		1	−31
7	1	7	13029.0564	2.0	2	4	12908.8164	2.0	2	−35	13023.4482		1	−17
7	1	6	13086.2667	1.1	3	−5	12974.0259[B]	0.3	2	−59	13079.5936[B]		1	−12
7	2	6	13087.8374	0.5	3	−2	12978.4231	1.5	2	−40	13082.0676	0.8	2	−64
7	2	5	13120.4161	4.7	4	−1	13011.8864	0.3	2	−65	13115.5826	1.2	2	−22
7	3	5	13140.8876	2.7	2	−10	13041.8451	1.2	2	−37	13137.2583	0.7	3	−22
7	3	4	13151.0826	0.8	3	−11	13052.6288		1	−56	13146.2595	1.8	3	−27
7	4	4	13199.4532	0.2	2	−15	13114.8913	0.1	3	7	13195.4566	2.8	3	−23

Note. N is the number of lines used for the upper energy level determination. σ (in 10^{-3} cm^{-1}) denotes the corresponding statistical error defined as the rms value of the deviation of the levels observed through several transitions. Δ represents the deviation of the observed levels from their calculated [12] values in 10^{-3} cm^{-1}. Energy levels marked with "B" or "T" were derived from blended lines or lines with tentative assignment, respectively (see text).

(*continued on next page*)

Table 2 (*continued*)

J	K_a	K_c	(401)				(321)				(500)			
			E_{obs}	σ	N	Δ	E_{obs}	σ	N	Δ	E_{obs}	σ	N	Δ
7	4	3	13200.5726	0.7	2	−14	13115.5485	1.7	3	−4				
7	5	3	13272.2592		1	−19	13204.1082		1	36	13268.2746	6.1	2	−31
7	5	2	13272.2986	2.4	3	−20	13204.0822	0.4	2	40				
7	6	2	13363.3119	0.6	2	−12	13309.4610	1.6	3	78				
7	6	1	13363.3118	0.4	2	−13	13309.4602	2.1	2	80				
7	7	1	13477.1995	1.0	2	13	13427.0034	2.1	2	76				
7	7	0	13477.1997	1.1	2	13	13427.0036	2.2	2	76				
8	0	8	13106.1243	0.5	2	−1	12986.1275	1.7	2	−32	13100.9756	2.9	2	−39
8	1	8	13106.2426	1.6	3	−2	12986.1865	5.2	2	−41	13167.2030		1	−19
8	1	7	13173.1788	1.6	3	−3	13063.7199	2.4	2	−46				
8	2	7	13173.7833	1.3	4	−5	13065.9871	2.0	2	−42	13167.9695	1.7	2	−25
8	2	6	13217.6605	1.5	4	−16	13111.7888	0.9	2	−72	13213.5585	2.1	2	−35
8	3	6	13232.5270	2.6	4	−13	13134.8550	1.3	2	−44	13229.5229	3.1	3	−26
8	3	5	13250.9151	3.2	2	−19	13153.2820	1.8	3	−62	13246.1256	1.8	2	−24
8	4	5	13293.2020	1.7	3	−21	13209.8081	1.9	3	−36	13289.4783	2.8	2	−37
8	4	4	13296.2474	0.6	3	−22	13211.6154	1.2	3	−23	13291.8039	2.8	3	−26
8	5	4	13366.0568		1	−29	13298.9936		1	33	13362.4177		1	−38
8	5	3	13366.2267		1	−34	13298.9524	4.7	2	28	13362.5619		1	−40
8	6	3	13457.1666	2.1	3	−27	13403.7019	2.7	2	62				
8	6	2	13457.1659	0.7	2	−30	13403.7055	0.4	2	66	13448.5338		1	−27
8	7	2	13571.4410	0.3	2	14	13520.8500	1.4	3	60				
8	7	1	13571.4408	0.3	2	12	13520.8499	1.6	3	59				
8	8	1					13649.9461		2	−14				
8	8	0					13649.9463	0.1	2	−14				
9	0	9	13192.1590		1	−85	13072.5704		1	−35	13186.7012[B]		1	−15
9	1	9	13192.3197	0.5	2	−2	13072.6358		1	−39	13186.6770		1	−30
9	1	8	13269.9083	1.7	4	−30	13161.9955	3.8	2	−52	13263.5157		1	−30
9	2	8	13269.2691	2.9	2	−11	13163.1825		1	−41	13263.1832	1.8	2	−36
9	2	7	13325.2007	0.4	4	−12	13221.1615		1	−97	13321.6313		1	−37
9	3	7	13334.6285	2.2	2	−22	13238.5693		1	−52	13332.4877	0.3	2	−21
9	3	6	13363.0087	0.8	2	−31	13266.9556	2.3	2	−57	13358.1275		1	−49
9	4	6	13398.5540	2.1	3	−28	13316.4060		1	−39	13395.1134	0.7	2	−45
9	4	5	13405.3713	2.8	2	−34	13320.5329	0.5	2	−59	13400.7979	3.8	2	−54
9	5	5	13471.8402		1	−39	13404.3332		1	−107	13468.4561	0.9	2	−61
9	5	4	13472.4127	1.5	2	−36	13406.0703	1.1	3	1	13468.9703	2.4	2	−52
9	6	4	13562.9912	0.9	2	−35	13509.8477		1	65	13558.0631	3.5	2	−55
9	6	3	13562.9995	3.0	2	−47	13509.8526	3.0	3	44				
9	7	3	13677.6353	6.1	2	1	13626.4864	1.8	2	46				
9	7	2	13677.6365	7.1	2	−5	13626.4864	1.5	2	46				
9	8	2					13756.5593	2.5	2	−36				
9	8	1					13756.5591	2.7	2	−37				
9	9	1					13866.9384		1	−36				
9	9	0					13866.9384		1	−36				
10	0	10	13287.4711	7.4	2	−6	13168.0197		1	−42				
10	1	10	13287.4627	3.3	3	−3	13167.1680		1	−266				
10	1	9	13373.6198	1.9	2	−16	13268.9688		1	−50	13367.6655		1	−26
10	2	9	13373.3404	1.0	2	−22	13270.0536		1	−50	13367.8570		1	−47
10	2	8	13444.0020	5.1	3	−36					13434.6863	1.8	2	−96
10	3	8	13446.9206	3.0	3	−29	13354.3151		1	−46	13438.2442	1.9	3	−49
10	3	7	13486.8983	6.5	2	−43					13482.1587	3.2	2	−68
10	4	7	13515.4363	4.1	3	−42	13434.3168	3.6	2	−48	13512.0057	3.7	2	−48
10	4	6	13528.1641	1.5	3	−57	13447.9677		1	−42				
10	5	6	13589.5775	1.3	2	−62	13522.8516	2.7	2	−3				
10	5	5	13591.1925	1.6	3	−59	13525.7387	0.1	2	−16	13587.3146		1	−47
10	6	5	13680.8281		1	−65	13627.9217	1.4	2	42				
10	6	4	13680.8912	4.3	2	−76	13627.9536		1	28				
10	7	4					13743.9277	0.1	2	35				
10	7	3					13743.9272	1.2	3	37				
10	8	3					13875.2783		1	−54				
10	8	2					13875.2784		1	−54				
10	9	2					13986.2095		1	−7				
10	9	1					13986.2101		1	−6				
10	10	1					14112.1937[B]		1	17				

Table 2 (*continued*)

J	K_a	K_c	(401)				(321)				(500)			
			E_{obs}	σ	N	Δ	E_{obs}	σ	N	Δ	E_{obs}	σ	N	Δ
10	10	0					14112.1937[B]		1	17				
11	0	11	13391.5780	0.5	2	−17	13269.8525		1	−187	13385.9523		1	−26
11	1	11	13391.5943		1	3	13271.4687[B]		1	−104	13385.9476		1	−30
11	1	10	13486.9642	1.9	3	−23								
11	2	10	13486.5708[B]	8.2	3	−54	13382.7770		1	−112				
11	2	9	13567.9624	4.0	2	−43								
11	3	9	13568.6913	4.1	3	−50	13478.2732		1	−91	13562.1699	3.5	2	−58
11	3	8	13621.2953	1.3	2	−63	13531.4966		1	−123	13616.8659		1	−80
11	4	8	13642.4644		1	−63	13561.6124[T]		1	−8	13639.9243	3.1	3	−62
11	4	7	13663.7467		1	−15	13583.7728	2.3	2	−97	13657.7327		1	−10
11	5	7	13719.1492		1	−85	13652.5987		1	1	13715.9257	2.6	2	−88
11	5	6	13722.9326	1.1	2	−77								
11	6	6	13810.7471		1	−90	13757.8924		1	6				
11	6	5	13810.8928	2.7	2	−93	13758.0639	1.3	2	7				
11	7	5					13873.1575		1	2				
11	7	4					13873.1599	0.2	2	−8				
11	8	4					14006.1613	5.7	2	−81				
11	8	3					14006.1609	6.1	2	−81				
11	9	3					14114.0778[T]		1	60				
11	9	2					14114.0777[T]		1	55				
12	0	12	13504.6584[B]		1	−24	13384.7587[B]		1	−101	13499.0428		1	−9
12	1	12	13504.6596	1.2	2	−16	13385.1954		1	−72	13499.0404		1	−11
12	1	11	13609.5272	0.2	2	−27	13511.2175[B]		1	−123				
12	2	11	13609.4651	1.5	3	−30	13508.2480[B]		1	−75				
12	2	10	13699.9199		1	−30								
12	3	10	13699.6742	1.2	2	−65	13612.7344		1	−97				
12	3	9	13765.0984	5.4	2	−72	13682.8099		1	−73	13761.1879		1	−88
12	4	9	13778.3974[T]		1	−54	13705.4024		1	−75	13778.4189		1	−67
12	4	8	13813.9163		1	−91					13799.5332		1	−30
12	5	8	13860.3312		1	−45								
12	5	7	13868.1220[B]		1	−104	13803.8320		1	−74				
12	6	7					13899.8213		1	−11				
12	7	6					14014.2477	4.5	2	−16				
13	0	13	13626.6775	0.6	2	−25	13506.9511		1	−35				
13	1	13	13626.6801	2.6	2	−18	13506.8988		1	−68				
13	1	12	13740.9415	0.8	2	−35								
13	2	12	13740.9008	1.6	2	−40								
13	2	11	13841.1159		1	−63	13756.7963		1	−108				
13	3	11	13841.0050		1	−64	13756.8430		1	−42				
13	3	10	13917.4789		1	−103								
13	4	10	13928.2174		1	−92	13855.5544[B]		1	−95	13927.4495	1.4	2	−109
13	4	9	13975.2617		1	−118								
13	5	9					13952.2258		1	−50				
13	6	8					14053.6746[T]		1	39				
13	7	6					14168.0323[T]		1	−1				
14	0	14	13757.6155	1.5	2	−29	13637.9459		1	−89				
14	1	14	13757.6168	0.4	2	−26	13637.9483		1	−89				
14	1	13	13881.2445		1	−36								
14	2	13	13881.2283		1	−43								
14	3	12	13990.5487		1	−70								
14	3	11	14084.8219		1	−107								
14	4	11	14086.1745		1	−108	14016.2705		1	−54				
14	5	10	14176.2805		1	−60								
14	5	9	14201.7366		1	−108								
14	6	9					14219.0082[T]		1	−47				
15	0	15	13897.4664		1	−56	13777.6714		1	−116				
15	1	15	13897.4670		1	−29	13777.6720[T]		1	−199				
15	1	14	14030.4816		1	−41	13934.5372[B]		1	−147				
15	2	14	14030.4918[B]		1	−60	13934.5826[T]		1	−131				
15	2	13	14151.1149		1	−59								
16	0	16	14046.1716		1	−41	13926.3536		1	−90				
16	1	16	14046.1718		1	−31	13926.3538		1	−130				

(*continued on next page*)

Table 2 (*continued*)

J	K_a	K_c	(401)				(321)				(500)			
			E_{obs}	σ	N	Δ	E_{obs}	σ	N	Δ	E_{obs}	σ	N	Δ
16	1	15	14188.5538[T]		1	29								
16	2	15	14188.4258		1	−57								
18	0	18	14370.0993		1	−48								
18	1	18	14370.0985		1	−72								
19	0	19	14545.2921		1	−51								
19	1	19	14545.2919		1	−49								

information relative to the highly excited vibrational states, their labeling is less reliable.

One drawback concerning the labeling of Ref. [12] is that no intensity considerations are taken into account. For instance, transitions belonging to rather strong bands (like (401)–(000) or (321)–(000)) may be attributed [12] erroneously as belonging to some 'exotic' highly excited bending states like (080), or even (0100) while transitions on such bending states are very weak and generally unobserved, except in the rare cases of strong resonance intensity transfer. It is well known that the ascribing of the rovibrational quantum numbers has to rely not only on the smooth variation of the (obs. − calc.) values versus the J values, but also on the line intensity values. In particular, the usual selection rules: $\Delta J = 0, \pm 1, \Delta K_a = 0, \pm 1, \pm 2, \ldots, \Delta K_c = 0, \pm 1, \pm 2 \ldots$ are valid for the rovibrational transitions, and, the smaller ΔK_a and ΔK_c values, the stronger the transition is. Such simple considerations show, for instance, that the (251) $10_{1\,10}$–10_{91} labeling given in Ref. [12] for the line observed at 12599.607 cm^{-1} is erroneous as transitions with $\Delta K_a = -8$, and $\Delta K_c = 9$ are much too weak to be observed. Our labeling for this transition is (142) 10_{82}–10_{91}.

In order to confirm our labeling, a series of energy levels calculations were performed in the frame of the effective Hamiltonian (EH) approach, considering each vibrational state as isolated. This procedure allowed for the attribution of a reliable label for the majority of the stronger transitions involving the (401), (321), and (500) upper states. However, we could not firmly establish the labeling for a number of rotational sublevels of the (142), (241), and (043) highly excited states for the few energy levels which, were observed through transitions borrowing their intensity from stronger line-resonance partners.

The full list of the 1025 D_2O lines corresponding to 1261 transitions is given in electronic form as Supplementary Material. It includes the measured line positions, the experimental and calculated [12] intensities and the rovibrational assignments of the upper and lower levels, if available. The 20 unassigned lines are also listed for completeness. They are all very weak and may possibly be due to the $D_2{}^{18}O$ isotopologue. Indeed if the oxygen atoms are in natural abundance in our sample, the $D_2{}^{18}O$ transitions are estimated to be weaker by a factor 500 compared to $D_2{}^{16}O$ transitions, which is comparable to the intensity ratio between the strongest and the weakest $D_2{}^{16}O$ transitions.

3.3. The problem of the assignment of the weakest lines

The assignment of the present high resolution D_2O spectrum was particularly difficult as we insisted on achieving the most complete and reliable identification list, including the weakest lines not included into CD relations. Indeed, in the case of the weakest lines, the usual criteria—small values and smooth variation of the (obs. − calc.) positions versus J and K_a, altogether with reasonable match between observed and calculated intensities—may not be sufficient and leave several equivalent possibilities for one weak experimental line. For example, the calculations give three transitions: (043) 3_{12}–2_{11} at 12742.438 cm^{-1}, (331) 5_{42}–4_{23} at 12742.580 cm^{-1}, and (420) 4_{14}–5_{05} at 12742.834 cm^{-1} which may correspond to the weak experimental line at 12742.602 cm^{-1}. The risk of an incorrect assignment is further increased for the weakest lines as: (i) the experimental uncertainty is larger both for position and for intensity, and (ii) the weakest transitions may involve a highly excited upper level affected by accidental resonance, and therefore, predicted with less accuracy. In case of local perturbations, the (obs. − calc.) values do not follow a regular variation, and may differ considerably in values and even in signs. This is particularly the case for the (142) state, for which a considerable number of the energy levels are involved in resonance interactions leading to an erratic variation of the residuals (see Fig. 6 and Table 2). As a result, we are less confident in those of our assignments attached to the weakest lines and we decided to leave a part of them unassigned. The label 'T'' (tentative assignment) marks the less reliable assignments both in Tables 2 and 3 and in the line list attached as Supplementary Material.

On the basis of the calculated [12] spectrum, the predicted lines missing in our experimental line list were examined. Taking into account all the transitions with a predicted intensity larger than 1.2×10^{-28} cm/mol—which corresponds approximately to our sensitivity—the unobserved absorption lines represent only 4% of the predicted integrated intensity in the studied spectral region. This 4% residual absorbance is mainly due to lines predicted in the

Table 3
$D_2{}^{16}O$ rovibrational energy levels of the (420), (222), (123), (043), (142), (302), (411), and (241) vibrational states derived from the ICLAS spectrum recorded between 12450 and 12850 cm^{-1}

VIB	*J*	K_a	K_c	E_{obs} (cm^{-1})	σ	*N*	Δ	VIB	*J*	K_a	K_c	E_{obs} (cm^{-1})	σ	*N*	Δ	VIB	*J*	K_a	K_c	E_{obs} (cm^{-1})	σ	*N*	Δ
420	3	2	2	12717.0161		1	−40	222	8	2	7	13247.7904		1	87	123	6	0	6	13216.8705		1	108
420	3	3	1	12770.5686		1	−4	222	8	4	4	13390.5465		1	63	123	6	1	6	13241.0644		1	81
420	4	2	3	12763.8658	0.9	2	−49	222	9	4	6	13496.3126		1	50	123	6	2	5	13274.3769		1	111
420	4	3	2	12818.1210		1	−12	222	10	1	9	13450.5424[B]		1	100	123	6	2	4	13279.4054		1	92
420	4	3	1	12818.4246		1	−22	222	10	6	4	13795.8282		1	−11	123	6	3	4	13342.6668		1	111
420	4	4	1	12891.6529		1	7	222	11	3	9	13667.0851		1	25	123	6	3	3	13343.0874		1	118
420	5	2	4	12816.1563	2.7	2	−52	222	11	4	8	13742.6973		1	−14	123	6	4	3	13227.9859[B]		1	110
420	5	3	3	12877.5964[B]		1	−54	043	3	3	1	12884.6716	2.1	2	−47	123	6	4	2	13225.1503		1	130
420	5	3	2	12878.8115		1	−37	043	3	3	0	12884.7321	2.8	2	−49	123	7	0	7	13288.4492		1	125
420	5	4	2	12951.2837		1	1	043	4	1	4	12814.7713		1	−52	123	7	1	7	13295.0566[B]		1	103
420	5	4	1	12951.1332		1	−6	043	4	3	2	12933.9072		1	−49	123	7	1	6	13331.2450		1	116
420	5	5	1	13047.8477		1	−3	043	4	3	1	12934.2953	2.4	3	−48	123	7	2	6	13358.0528		1	91
420	5	5	0	13047.8420		1	−18	043	5	0	5	12863.2187		1	3	123	7	2	5	13429.0419		1	111
420	6	3	4	12948.9517		1	−45	043	5	3	3	12994.9661	5.3	2	−57	123	7	3	5	13301.7172		1	111
420	6	4	3	13022.9973		1	−32	043	5	3	2	12996.4273	0.1	2	−47	123	7	4	3	13304.0055		1	114
420	6	4	2	13023.0673	0.4	2	−30	043	6	3	4	13068.2365[B]		1	−61	123	8	0	8	13383.0921[B]		1	135
420	7	3	5	13032.3723	0.7	3	−21	043	6	3	3	13072.1948[B]		1	−62	123	8	1	8	13388.2997[B]		1	90
420	7	4	4	13106.8520		1	−40	043	6	6	1	13381.7263[T]		1	−81	123	8	2	7	13588.0931		1	102
420	7	4	3	13107.2089		1	−34	043	6	6	0	13381.7262[T]		1	−81	123	9	1	9	13640.6226		1	102
420	7	6	2	13327.6218		1	6	043	7	2	5	13113.9252	2.8	2	−46	123	10	1	10	13434.4184		1	99
420	7	6	1	13327.6161		1	4	043	7	5	3	13341.9810[B]		1	−4	302	4	3	1	13178.7500		1	120
420	8	2	6	13098.7965	2.1	2	−101	043	7	5	2	13341.9811		1	−19	302	4	4	1	13235.1353[B]		1	127
420	8	3	6	13127.0153	4.4	2	−72	043	8	2	6	13218.7671	1.3	2	−47	302	4	4	0	13235.1347		1	153
420	8	3	5	13140.4060		1	−105	043	8	5	4	13438.6589		1	−35	302	6	2	4	13279.0808		1	119
420	8	4	5	13202.7584		1	−82	043	9	2	8	13265.8701		1	−52	302	6	3	3	13310.2857		1	112
420	8	4	4	13204.0313[B]		1	−74	043	9	2	7	13334.0100		1	−20	302	8	2	6	13464.9816		1	136
420	8	5	4	13286.2269		1	−21	043	9	5	4	13547.5816		1	−52	302	8	5	4	13604.3459		1	15
420	8	5	3	13286.4833		1	−19	043	10	1	9	13370.8938		1	−72	302	8	5	3	13604.3458		1	18
420	9	3	7	13233.3390	4.4	2	−75	043	10	2	9	13374.7816	3.0	2	−69	302	9	1	8	13513.7795		1	100
420	9	4	6	13310.6578		1	−77	043	11	2	10	13487.8205		1	−84	302	9	2	8	13514.6863		1	113
420	9	4	5	13313.7433[B]		1	−102	043	11	3	8	13657.9683		1	−41	302	10	0	10	13532.4969		1	106
420	9	5	5	13393.8344		1	−35	142	5	3	2	12834.5025		1	−128	302	10	1	10	13532.3392		1	113
420	9	5	4	13394.4030[B]		1	−57	142	5	5	1	13030.8572		1	20	302	10	1	9	13618.6544[B]		1	132
222	1	0	1	12810.9173[B]		1	130	142	5	5	0	13030.8515		1	12	302	11	1	11	13636.3486		1	110
222	1	1	1	12820.2316[B]		1	120	142	6	5	2	13099.2457		1	−17	302	12	0	12	13749.3643		1	119
222	2	0	2	12833.6917	1.3	2	97	142	6	5	1	13099.2458		1	−26	302	12	1	12	13749.3619		1	92
222	3	0	3	12866.7830	3.1	2	120	142	7	4	4	13081.2905	2.2	2	−42	302	13	0	13	13871.4290		1	106
222	3	1	3	12871.5346		1	106	142	7	5	3	13181.3567		1	−24	302	13	1	13	13871.4283		1	93
222	3	1	2	12887.4355		1	107	142	7	6	2	13301.3177[T]		1	129	241	5	4	1	12778.1430		1	−41
222	3	2	2	12911.6143		1	116	142	7	7	1	13419.6798		1	103	241	6	5	2	12966.1902		1	−57
222	4	0	4	12909.2003[B]		1	120	142	7	7	0	13419.6797		1	109	241	6	5	1	12966.5939		1	−71
222	4	3	1	13012.1322	0.6	2	139	142	8	6	3	13421.8686[T]		1	−2	241	7	5	2	13048.1994	9.0	3	−106
222	5	0	5	12960.4515		1	105	142	8	6	2	13421.8345[T]		1	−17	241	8	5	3	13144.0349		1	−108
222	5	1	5	12962.0200	4.5	6	103	142	8	7	2	13514.3261		1	83	241	9	9	1	13820.2104		1	−116
222	5	2	4	13014.9806[B]		1	100	142	8	7	1	13514.3257		1	101	241	9	9	0	13820.2104		1	−131
222	5	2	3	13028.1738		1	85	142	9	3	7	13192.4517	1.2	2	212	241	10	3	8	13168.8790[T]		1	−203
222	6	4	3	13213.9008		1	120	142	9	7	3	13620.8259		1	67	241	12	6	7	13780.7809	9.4	2	−96

(*continued on next page*)

Table 3 (*continued*)

VIB	*J*	K_a	K_c	E_{obs} (cm^{-1})	σ	*N*	Δ	VIB	*J*	K_a	K_c	E_{obs} (cm^{-1})	σ	*N*	Δ	VIB	*J*	K_a	K_c	E_{obs} (cm^{-1})	σ	*N*	Δ
222	6	4	2	13213.5093		1	143	142	9	7	2	13620.8217[B]		1	85	411	2	1	2	13915.9795[B]		1	1
222	7	0	7	13089.1748		1	98	142	10	5	5	13514.1895	1.8	2	−77	411	3	0	3	13942.8516		1	−26
222	7	1	7	13089.4674		1	98	142	10	8	3	13982.3951		1	−64	411	4	1	4	13986.3163		1	−59
222	7	2	5	13196.5991	0.5	2	−18	142	10	8	2	13982.3945		1	−64	411	5	0	5	14034.9944		1	−10
222	7	3	5	13222.0064		1	111	142	11	4	8	13540.6596[T]		1	−2	411	7	0	7	14162.2498[B]		1	−20
222	7	4	4	13296.4612		1	93	142	11	5	7	13669.3521		1	−52	411	8	1	8	14238.6243[T]		1	−80
222	8	1	8	13166.9317		1	78	123	6	0	6	13156.2132		1	108	411	9	0	9	14324.1277		1	−80
222	8	1	7	13243.9114		1	60	123	6	1	6	13156.4122		1	81								

Note. *N* is the number of lines used for the upper energy level determination. σ (in 10^{-3} cm^{-1}) denotes the corresponding statistical error defined as the rms value of the deviation of the levels observed through several transitions. Δ represents the deviation of the observed levels from their calculated [12] values in 10^{-3} cm^{-1}. Energy levels marked with "B" or "T" were derived from blended lines or lines with tentative assignment, respectively (see text).

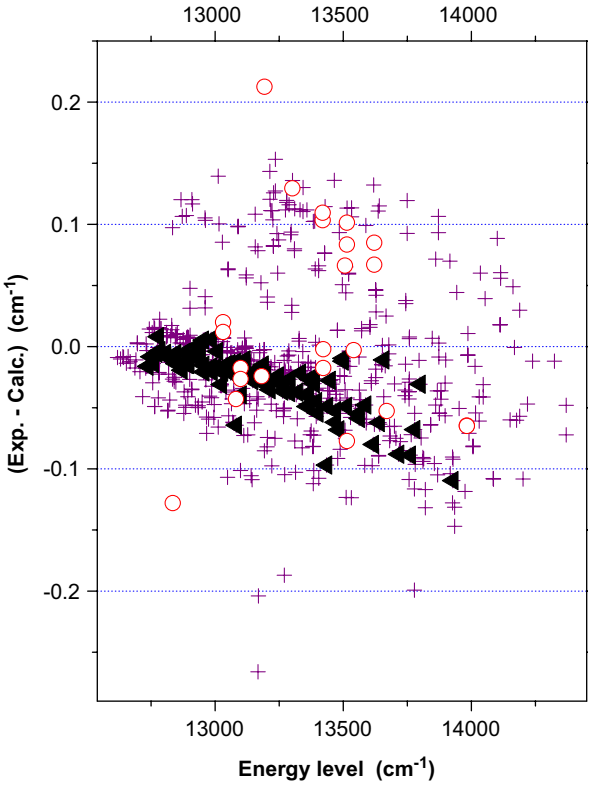

Fig. 6. Variation of the difference between the experimental and calculated energy levels versus the energy level value. The full triangles and open circles are relative to the (005) and (142) states, respectively, while crosses correspond to the nine other vibrational states. The dispersion of the deviation values of the (142) state is the result of resonance interactions with other vibrational states (see text).

12650–12820 cm^{-1} region which could not be experimentally observed, as they are superimposed on much stronger D_2O lines.

4. Discussion

Among the valuable information retrieved from our analysis is the first determination of the origins for the (321)–(000), (500)–(000), (222)–(000), (123)–(000), and (302)–(000) bands, which were either obtained from observed transitions reaching the 0_{00} level or extrapolated from the (obs. − calc.) variation for the *J*0*J* energy levels with an accuracy better than 0.1 cm^{-1} (see Table 1).

Analysis within the effective Hamiltonian (EH) approach reported in Ref. [2] deserves to be commented on. Six vibrational states were involved into a simultaneous fitting to reproduce 63, 2, and 6 energy levels of the (401), (321), and (302) states, respectively. This demonstrates clearly the difficulties encountered in the EH approach when dealing with highly excited vibrational states of the water molecule. Despite the fact that most of the rotational parameters of the dark states were reasonably well extrapolated from the lower lying polyads and kept fixed in the

fitting of Ref. [2], the variation of 28 rotational and resonance constants were necessary to reproduce 71 energy levels. Furthermore, differences as large as 25.8 cm^{-1} are noted for the vibrational term values evaluated in [2] compared with our experimental values or those accurately predicted in [12]. Five of the experimental energy levels reported in [2] are not confirmed.

5. Conclusion

The high resolution absorption spectrum of the D_2O molecule has been recorded by means of the high sensitive ICLAS technique in the 12485–12853 cm^{-1} region and identified using the results of the most accurate available variational calculations of the D_2O spectrum [12]. The typical sensitivity achieved allowed for the detection of transitions with intensity values as low as 2×10^{-28} cm/molecule. This detection limit is about 100 times lower that those achieved in the same spectral region by ICLAS with a FTS detection scheme or by FTS with a 600 m path length. A set of 586 energy levels belonging to 11 vibrational states was derived, while only 85 energy levels, mostly of the (4 0 1) state, were available from previous studies [2,3].

In the considered spectral range, the difficulties of vibrational assignment are much larger in the case of the D_2O isotopologue than for the H_2O and HDO species. This may be partly due to the fact that the 12500 cm^{-1} region is the highest spectral region analyzed so far for the D_2O species. Therefore, the determined energy levels, which were found to deviate from the predicted values by up to -0.27 cm^{-1}, will be useful for a further refinement of the D_2O PES.

The problem of the ascribing vibrational and rotational quantum numbers for the highly excited rovibrational states of D_2O has been discussed and the difficulties in the weak lines assignment were outlined. Concerning the labeling provided in Ref. [12], we can draw the conclusion that the used automatic procedure which considered only the energy level values, should be supplemented by considering the wavefunction and/or the intensity of the corresponding transitions. Nevertheless, most of the proposed rovibrational labeling was supported by theoretical considerations, in particular effective Hamiltonian calculations, and will be valuable for ascribing the quantum numbers in future high accuracy variational calculations of the D_2O line positions.

Acknowledgments

We thank Alain Jenouvier (GSMA, Reims) for providing the D_2O FTS line list of Ref. [3], prior to publication. The present work, performed in the frame of the European research network QUASAAR (MRTN-CT-2004-512202), is jointly supported by the INTAS foundation (Project 03-51-3394) as well as a collaborative project between CNRS and RFBR (PICS Grant No. 05-05-22001) and the Russian Foundation for Basic Research. The study was performed as part of the IUPAC task group 2004-035-1-100 on "A database of water transitions from experiment and theory". A.C. (Grenoble) is grateful for the financial support provided by Programme National LEFE of CNRS (INSU).

Appendix A. Supplementary data

Supplementary data for this article are available on ScienceDirect (www.sciencedirect.com) and as part of the Ohio State University Molecular Spectroscopy Archives (http://msa.lib.ohio-state.edu/jmsa_hp.htm).

References

[1] O.V. Naumenko, F. Mazzotti, O.M. Leshchishina, J. Tennyson, A. Campargue, J. Mol. Spectrosc. 242 (2007) 1–9.
[2] S.M. Hu, O.N. Ulenikov, E.S. Bekhtereva, G.A. Onopenko, Sheng-Gui He, Hai Lin, Ji-Xin Cheng, Qing-Shi Zhu, J. Mol. Spectrosc. 212 (2002) 89–95.
[3] A. Jenouvrier, S. Fally, A.C. Vandaele, O.V. Naumenko, O. Leshchishina, S. Shirin, J. Tennyson, J. Mol. Spectrosc., submitted for publication.
[4] A. Charvat, A.A. Kachanov, A. Campargue, D. Permogorov, F. Stoeckel, Chem. Phys. Lett. 14 (1993) 495–501.
[5] A. Kachanov, A. Charvat, F. Stoeckel, J. Opt. Soc. Am. B 11 (1994) 2412–2419.
[6] S. Hu, A. Campargue, Z.-Y. Wu, Y. Ding, A.-W. Liu, Q.-S. Zhu, Chem. Phys. Lett. 372 (2003) 659–667.
[7] R.N. Tolchenov, J. Tennyson, J.W. Brault, A.A.D. Canas, R. Shermaul, J. Mol. Spectrosc. 215 (2002) 269–274.
[8] M. Bach, S. Fally, P.-F. Coheur, M. Carleer, A. Jenouvrier, A.C. Vandaele, J. Mol. Spectrosc. 232 (2005) 341–350.
[9] S.V. Shirin, N.F. Zobov, O.L. Polyansky, J. Tennyson, T. Parekunnel, P.F. Bernath, J. Chem. Phys. 120 (2004) 206–210.
[10] D.W. Schwenke, H. Partridge, J. Chem. Phys. 113 (2000) 6592–6597.
[11] H. Partridge, D.W. Schwenke, J. Chem. Phys. 106 (1997) 4618–4639.
[12] S.V. Shirin, N.F. Zobov, O.L. Polyansky, J. Quant. Spectrosc. Radiat. Transfer, in press, doi:10.1016/j.jqsrt.2007.07.010.
[13] P. Barletta, S.V. Shirin, N.F. Zobov, O.L. Polyansky, J. Tennyson, E.F. Valeev, A.G. Csaszar, J. Chem. Phys. 125 (2006) 1–18.
[14] N.F. Zobov, R.I. Ovsyannikov, S.V. Shirin, O.L. Polyansky, Opt. Spectrosc. 102 (N3) (2007) 348–353.